Journal of Nematology 27(2):135–142. 1995.

The Immunofluorescent Localization of Subventral Pharyngeal Gland Epitopes of Preparasitic Juveniles of *Heterodera glycines* Using Laser Scanning Confocal Microscopy

WILLIAM G. T. WILLATS,[1,2] HOWARD J. ATKINSON,[1] AND ROLAND N. PERRY[2]

Abstract: Laser scanning confocal microscopy (LSCM) was used to localize the reactivity of a monoclonal antibody (Sv2) that binds to the subventral pharyngeal glands of preparasitic juveniles of *Heterodera glycines*. The greater resolution, magnification, and image analysis of LSCM compared with conventional epifluorescent microscopy enabled Sv2 binding to be localized much more precisely to the periphery of the secretory granules. A linear increase of about 55% in fluorescent intensity was found over a 23-μm length of subventral pharyngeal gland just distal to the terminal ampullae. LSCM is a rapid and effective technique for precise immunolocalization of epitopes.

Key words: confocal microscopy, *Heterodera glycines*, nematode, monoclonal antibody, secretory granule, subventral pharyngeal gland.

Cyst and root-knot nematodes possess one dorsal and two subventral pharyngeal glands that produce membrane-bound secretory granules and play a central role in parasitism (11,13). In *Globodera rostochiensis*, the pharyngeal glands appear not to be involved in hatching, and accumulation of secretory granules in the glands in response to host root diffusate may prepare juveniles for a feeding phase after hatching (18). The subventral glands in *Heterodera glycines* are active during establishment within roots and may be involved in the transformation of the intestine into an absorptive organ (3). The timing of gland activity in *Meloidogyne incognita* suggests a role in invasion and migration (26).

Some characterization of the secretory contents of pharyngeal gland cells has been achieved by histochemistry and microspectrophotometry (4), ultrastructural cytochemistry (22), and analysis of secretions released from animals in aqueous solutions (11). In recent years monoclonal antibodies (MAbs) have been shown to have considerable potential as probes for the study of various components of the secretory granules (12).

Received for publication 23 May 1994.

[1] Centre for Plant Biochemistry and Biotechnology, The University of Leeds, Leeds, LS2 9JT, UK.

[2] Entomology and Nematology Department, IACR, Rothamsted Experimental Station, Harpenden, Herts., AL5 2JQ, UK.

An important step in the establishment of a MAb probe is the localization of antigen binding by indirect immunolabelling. Stage-specific MAb reactivity has been defined in the dorsal and subventral pharyngeal glands of *H. glycines* (2) and *M. incognita* (7) using conventional epifluorescence microscopy. Using electron microscopy, MAb specificity has been established at the ultrastructural level in *M. incognita* secretory granules (13). The latter approach offers much more precise localization than is possible using indirect conventional epifluorescence microscopy but requires complex sample preparation and does not allow study of in toto mounts.

Laser scanning confocal microscopy (LSCM) is a recently developed technique (24) that considerably widens the scope of immunofluorescent research (21). It offers greater resolution than is possible with conventional epifluorescence microscopy, while lacking the above-mentioned limitations of electron microscopy. In LSCM a beam of laser light is focused on a single point, or voxel. Fluorescence emission excited within the voxel is focused onto a photo detector. A complete two-dimensional image is compiled point by point as the beam scans across the specimen. As only one point in the focal plane is illuminated with full intensity at any one time, contributions to the signal from flare, scattered light, and autofluorescence are greatly reduced. An aperture at a position

confocal with the voxel ensures that light emitted by any region above or below the focal plane fails to reach the detector and out-of-focus blur is virtually eliminated. Furthermore, because the total energy deposited on the specimen is less than in conventional microscopy, the rate of fluorescence photo bleaching is reduced (25).

Noninvasive serial optical sections can be obtained up to 500 μm deep within a specimen by controlled adjustments to the focal plane. This allows the generation of complete in-focus 3D data sets (5). Digital image processing and image storage allow a variety of complex image manipulations, including the generation of stereoscopic images (23) and animated sequences (21).

We examined the potential of LSCM to determine the precise location of the reactivity of Sv2, a MAb previously observed by conventional epifluorescent microscopy and reported to bind to the subventral glands of *H. glycines* (3). The two approaches were compared to determine if the superior resolving ability of LSCM assisted by image analysis could provide information previously possible only by using immunoelectron microscopy.

Materials and Methods

Indirect immunofluorescent labeling: A fluorescein isothiocyanate (FITC) conjugated second antibody was used to visualize the antisubventral gland MAb Sv2 in fragments of second-stage juveniles (J2) of *H. glycines*. The method used was a modification of that used by Atkinson et al. (2). All incubations were in microcentrifugation tubes, and all centrifugations were at 2,000*g*.

Freshly hatched (<48 hours old) J2 of *H. glycines* (Ra3) were fixed overnight in picric acid formaldehyde (PAF) with 0.1M sucrose at 4 C. After fixing, the nematodes were centrifuged, the PAF carefully removed using a Pasteur pipette connected to a vacuum pump, and the nematode pellet transferred to a clean glass plate. Using a razor blade, worms were cut into fragments approximately 60 μm long. Fragments were then fixed for 5 hours in PAF before being washed three times in M9 buffer. The fragments were incubated in 4 mg/ml proteinase K (Sigma, UK) for 20 minutes before freezing at −50 C for 20 minutes. After thawing, fragments were treated for 1 minute in methanol and 2 minutes in acetone, both at −20 C, then incubated in 1mM phenylmethylsulphonyl fluoride (PMSF) with 2% bovine serum albumen (BSA) in phosphate buffered saline (PBS) for 30 minutes.

Fragments were washed five times in PBS and incubated overnight at 4 C on an orbital shaker in primary antibody (Sv2), diluted 1:300 in PBS containing 1% BSA and 0.2% Triton X-100. Positive control fragments were incubated under the same conditions in an antibody that reacted with the neuropeptide FMRFamide. Negative control fragments were incubated only in second antibody conjugate. Fragments were recovered by centrifugation and washed extensively in PBS.

Primary antibody was detected by incubating fragments in FITC-conjugated IgG goat anti-mouse (whole molecule) (Sigma, UK) diluted 1/300 in Tris buffered saline (TBS) with 3% BSA and 0.2% Triton X-100 for 5 hours at room temperature. Fragments were then washed five times in PBS and twice in double-distilled deionized water. After the final wash, most of the water was removed and fragment pellets were transferred to acetone-cleaned multiwell slides (ICN-Flow). Any remaining water was removed by using a finely drawn-out Pasteur pipette connected to a vacuum pump. A drop of anti-quenching agent was placed on each well, and slides were covered with acetone-cleaned cover slips.

Visualization of bound antibodies: Conventional epifluorescent microscopy: Specimens were viewed at magnifications up to ×1,000 using a microscope with an epifluorescent attachment (Olympus BH-2) fitted with a 455-nm excitation filter and a 460-nm secondary filter. Micrographs were taken using a camera (Olympus

OM4) and color reversal film (Kodacolor Gold, ASA 400).

Visualization of bound antibodies: Laser scanning confocal microscopy: Specimens were viewed using a laser-scanning confocal microscope (Bio Rad MRC-600 series). Images were electronically stored and manipulated. Prints were obtained using a video printer (Sony). Selected prints were subsequently analyzed using an image analyzer (Data Translation).

Results

Conventional epifluorescent microscopy: In positive controls treated with the anti-FMRFamide primary antibody, fluorescence of neurones was seen at ×400 magnification. Only nonspecific binding to cut ends and autofluorescence were observed in negative control fragments that were treated with secondary antibody only (not shown).

At low magnification, highly specific intense fluorescence was seen in the subventral glands of *H. glycines* fragments incubated in Sv2 primary antibody (Fig. 1A,B,C). Weak cross reactivity to the dorsal gland duct (Fig. 1C) and some autofluorescence, particularly from the cephalic framework (Fig. 1B,C), were observed in most fragments. All the fragments examined (approximately 100) that contained whole or parts of subventral glands showed a similar pattern of reactivity. At ×1,000 magnification, a granular distribution of Sv2 binding was seen in gland lobes, although reactivity could not be discerned on discrete regions of granules (Fig. 1D).

Laser scanning confocal microscopy: The greater resolution, magnification, and image analysis available with confocal microscopy enabled Sv2 binding to be localized much more precisely. At low magnification both gland lodes, their ducts, and terminal ampullae were clearly visible in fragments incubated in Sv2 (Fig. 2A). Weak cross reactivity with the excretory system was observed in some fragments (Fig. 2B). Reactivity was not uniform in intensity, being most intense near the point of antibody entry (the cut ends of fragments) and also intense in terminal ampullae, regardless of their proximity to cut ends (Figs. 1B,2A). A profile of this change in fluorescence was generated by image analysis (Fig. 2C). It established a linear increase of about 55% in fluorescent intensity over a 23-μm length of subventral pharyngeal gland just distal to the terminal ampullae. Fluorescence in the ampullae themselves could not be quantified because the intensity in this region saturated the image. In most fragments fluorescence was weak in the anterior portion of gland lobes, and regions of antibody binding could not be defined (Figs. 2A,B).

At high magnification, numerous granules ranging in size from about 0.5 μm to 1 μm were visible in the posterior portion of subventral gland lobes. A ring-like pattern of fluorescence revealed that Sv2 reactivity was confined to the periphery of these granules (Fig. 3A,B). This pattern of reactivity was confirmed by taking optical sections through granules. A series of longitudinal optical sections was also taken through the entire width of glands, with little loss of resolution or image intensity. These sections established that granules were evenly distributed within the gland lobes. By electronically combining these sections with transverse sections, a 3D image was generated that could be rotated and viewed through 360 C (not shown). Optical sectioning through subventral gland ducts revealed a population of smaller granules in this region of less than 0.5 μm in diameter, but reactivity could not be discerned as being confined to the granule periphery.

Discussion

The autofluorescence seen in most fragments, particularly around the cephalic framework, is common in nematodes (2,10) and could be distinguished readily by color from specific FITC fluorescence. Conventional epifluorescent microscopy confirmed that Sv2 bound specifically to the subventral pharyngeal glands of J2 of

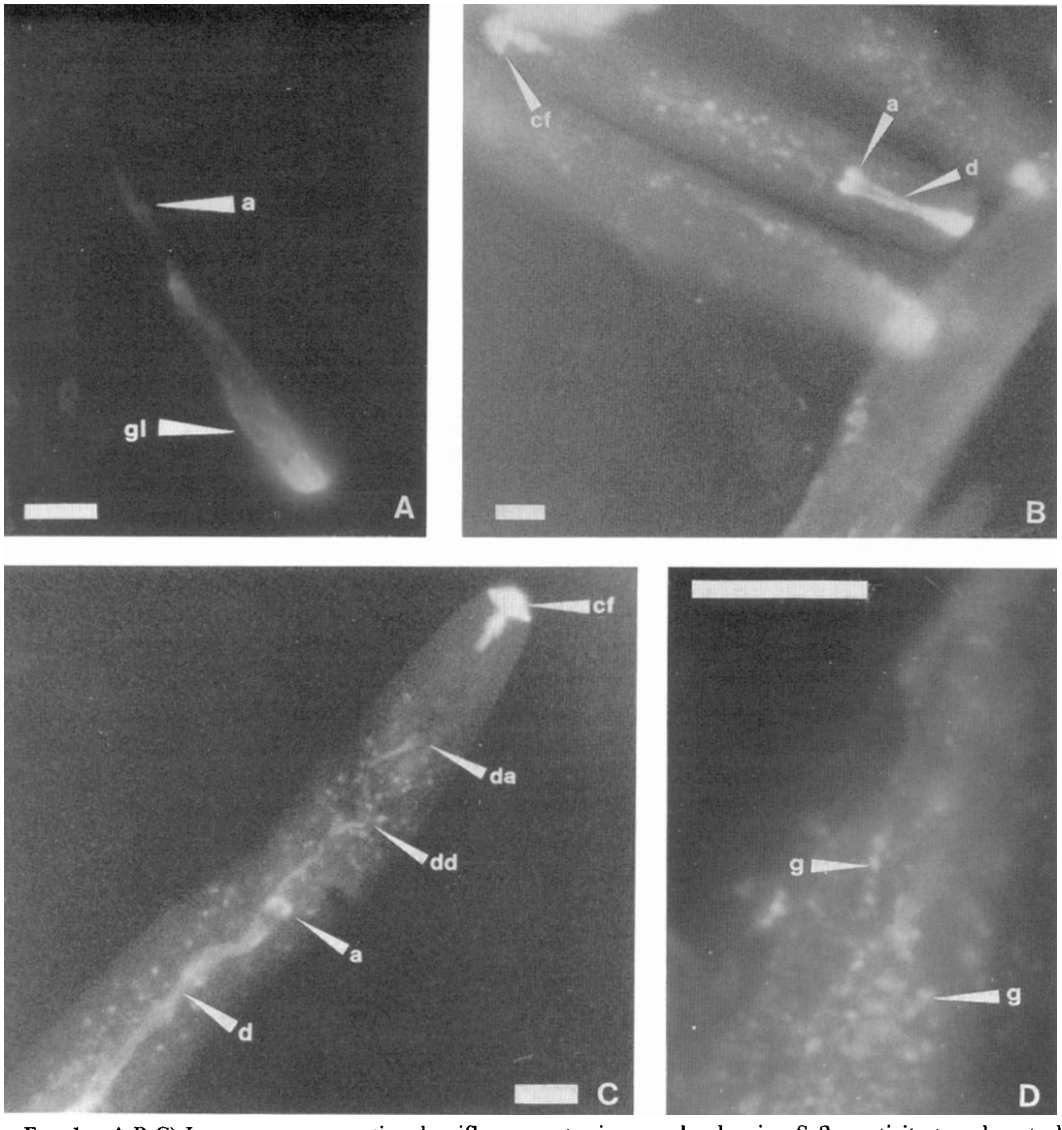

FIG. 1. A,B,C) Low-power conventional epifluorescent micrographs showing Sv2 reactivity to subventral glands of J2 *H. glycines*. cf = cephalic framework; a = subventral gland ampulla; gl = subventral gland lobe; d = subventral gland duct; dd = dorsal gland duct; da = dorsal gland ampullae. D) High-power conventional epifluorescent micrograph showing Sv2 binding to subventral gland granules (g) of J2 *H. glycines*. Scale bars = 10 μm.

H. glycines, with some weak cross reactivity to dorsal pharyngeal gland ducts and occasionally the excretory-secretory system. Inter-gland cross reactivity has been reported in similar experiments with *M. incognita* (14), suggesting that there may be some similarities in the antigens recovered from the two types of pharyngeal glands.

The enhanced resolution and magnification available with LSCM, complemented by image manipulation software, greatly increased the information available from the same set of specimens as those used for conventional epifluorescent microscopy. LSCM provided an overview of Sv2 binding at low magnification and localized reactivity to discrete granule domains at high magnification.

In the posterior portion of subventral gland lobes, Sv2 was predominantly con-

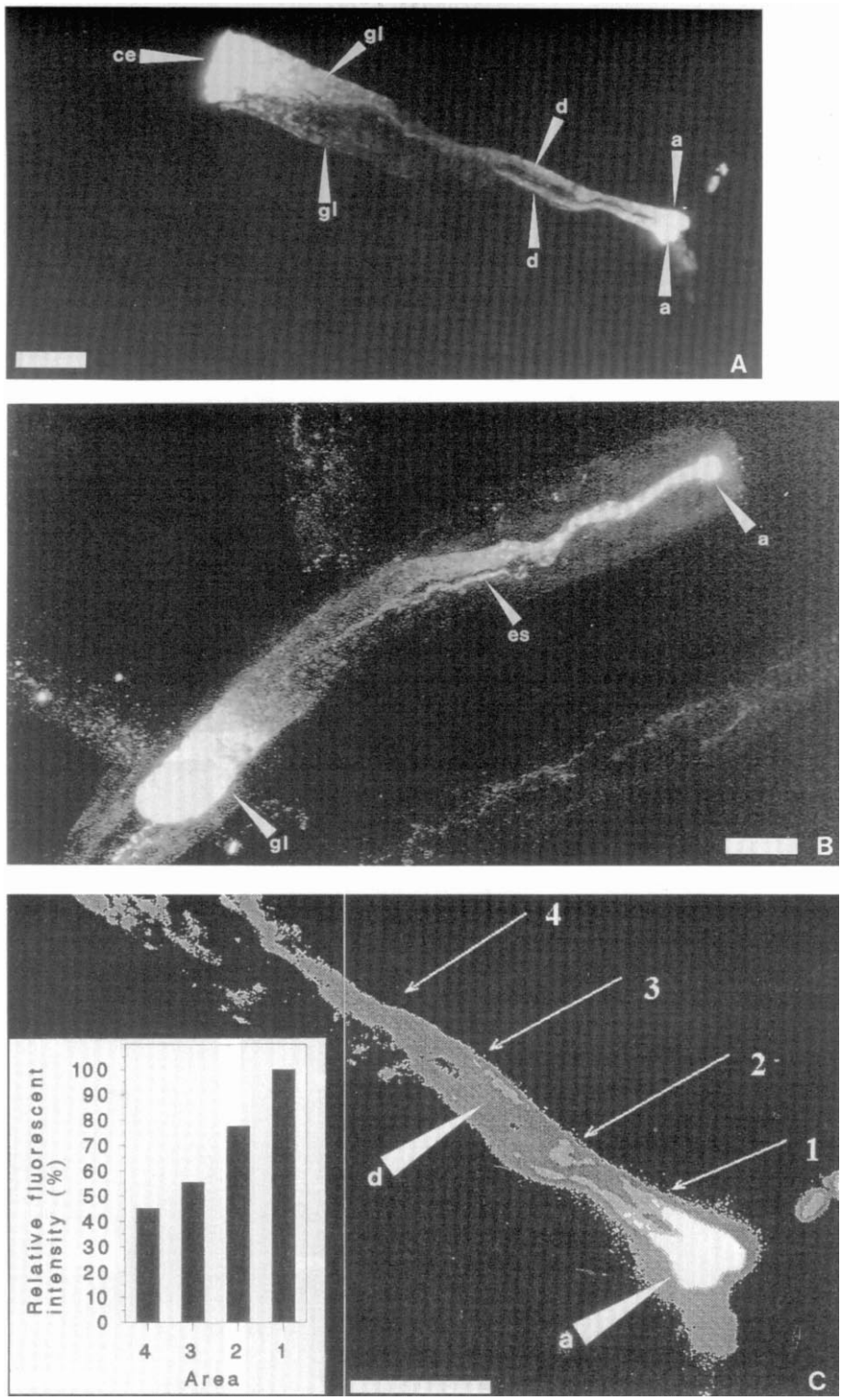

FIG. 2. A,B) Low-power laser scanning confocal microscope (LSCM) micrographs showing Sv2 binding to the subventral glands of J2 *H. glycines*. a = ampullae; d = duct; gl = gland lobe; ce = cut end; es = secretory system. C) Image analysis of duct (d) and ampullae (a) portion of gland shown in Fig. 2A, showing a linear increase in relative fluorescent intensity toward the ampullae. Scale bars 10 μm.

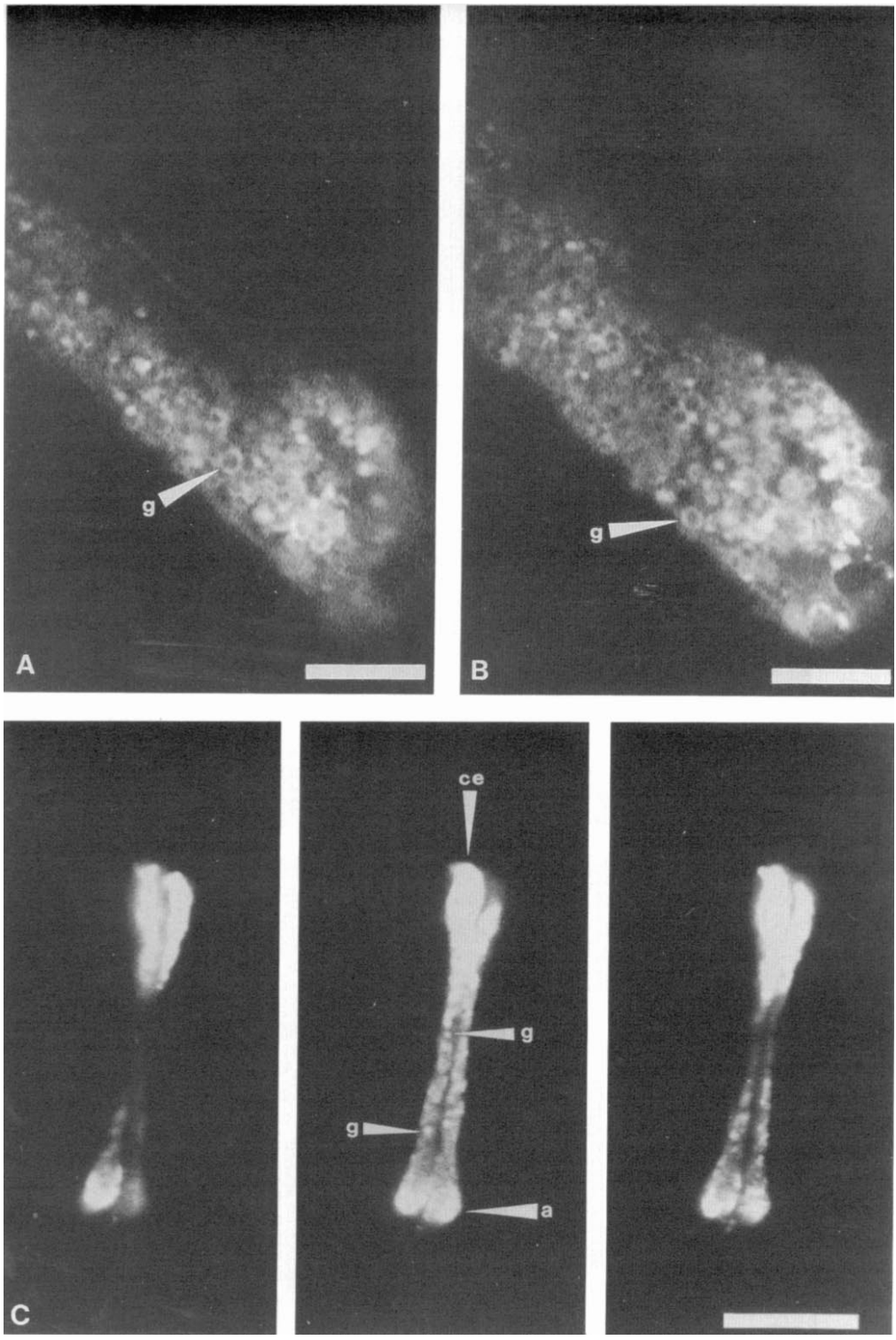

FIG. 3. A,B) High-power LSCM optical serial sections 1 μm apart through a subventral gland lobe of a J2 *H. glycines* showing Sv2 binding to the outer portion of secretory granules and the distribution of granules within the gland lobe. Scale bar = 5 μm. C) High-power LSCM optical serial sections through the ampullae (a) and duct region of a subventral gland of J2 *H. glycines,* showing Sv2 binding to a population of granules (g) less than 0.5 μm in diameter. a = ampullae; ce = cut end. Scale bar = 10 μm.

fined to the periphery of secretory granules. This pattern of reactivity is unlikely to arise merely from the physical exclusion from the granule core, as antibodies are known to be able to penetrate the interior of secretory granules of *M. incognita* (14). It seems more likely that it reflects granule organization. Ultrastructural studies have shown that secretory granules formed in this region of the subventral gland cells of preparasitic *M. incognita* subventral gland cell have two distinct domains, a central core surrounded by a peripheral matrix (13).

Other studies on various cell systems indicate that the peripheral region of secretory granules is important in controlling exocytosis (16) and in directed granule transport, which may be in association with microtubules (15) or microfilaments (1,20). A microtubule array has been reported in both dorsal and subventral gland extensions (8) and may be part of such a granule transport system.

Reactivity of Sv2 in the anterior portion of the subventral gland lobes was very weak, and it was not possible to localize binding in this region. This diminished reactivity is probably not due to inaccessibility to the antibody because the ampullae fluoresced very intensely, even when farthest from the point of antibody entry.

The increase in fluorescence within the ampullae of more than double that in the ducts over a distance of only 23 μm probably represents an increase in epitope concentration. It may arise from continued reactivity with granules after release of their contents, or to reactivity to recycling membranous vesicles. During exocytosis, granule membrane is added to cell membrane but is subsequently recovered by endocytosis back into the secretory cell (6). The resultant empty membranous vesicles may be recycled back to the trans Golgi complex (19). Electron microscopy studies suggest that this mechanism operates in nematode pharyngeal gland cells (13). Therefore, the high level of Sv2 reactivity in this region could be due to the presence of membrane associated with both unspent granules and reformed vesicles.

Changes in granule size may be related to conformational changes associated with control of granule discharge (17). In vitro studies indicate that secretory granules may undergo repeated cycles of condensation and decondensation without losing their original shape (9). We envisage that LSCM analysis of granule size and patterns of MAb reactivity may determine granule passage and discriminate between phases of secretory activity, involving predominance of either unspent granules or reformed membranous vesicles.

This work has shown confocal microscopy to be a rapid and effective technique for precise immunolocalization of epitopes. It increases the scope of nematode immunofluorescence research and allows localization of a MAb to discrete domains on individual secretory granules. The approach provides an improved basis for studying changes in granule production and use during invasion, establishment, and development of plant-parasitic nematodes.

Literature Cited

1. Adams, R. J., and T. D. Pollard. 1989. Binding of Myosin I to membrane lipids. Nature 340:565–568.

2. Atkinson, H. J., P. D. Harris, E. J. Halk, C. Novitski, J. Leighton-Sands, P. Nolan, and P. C. Fox. 1988. Monoclonal antibodies to the soya bean cyst nematode, *Heterodera glycines*. Annals of Applied Biology 112:459–469.

3. Atkinson, H. J., and P. D. Harris. 1989. Changes in nematode antigens recognised by monoclonal antibodies during early infection of soya beans with the cyst nematode *Heterodera glycines*. Parasitology 98:479–487.

4. Bird, A. F., and W. Sauer. 1967. Changes associated with parasitism in nematodes. II. Histochemical and microspectrophotometric analysis of preparasitic and parasitic larvae of *Meloidogyne javanica*. Journal of Parasitology 53:1262–1269.

5. Brakenhoff, G. J., H. T. M. Van de Voort, E. A. Van Spronsen, and N. Nanninga. 1989. Three-dimensional imaging in fluorescence by confocal scanning microscopy. Journal of Microscopy 153: 151–159.

6. Burgess, T. L., and R. B. Kelly. 1987. Constitutive and regulated secretion of proteins. Annual Review of Cell Biology 3:243–293.

7. Davis, E. L., R. Allen, and R. S. Hussey. 1994. Developmental expression of esophageal gland antigens and their detection in stylet secretions of *Meloidogyne incognita*. Fundamental and Applied Nematology 17:255–262.

8. Endo, B. Y. 1984. Ultrastructure of the esophagus of larvae of the soybean cyst nematode, *Heterodera glycines*. Proceedings of the Helminthological Society of Washington 51:1–24.

9. Fernandez, J. M., M. Villalón, and P. Verdugo. 1991. Reversible condensation of mast cell secretory products in vitro. Biophysical Journal 59:1022–1027.

10. Forge, T. A., and A. E. MacGuidwin, 1989. Nematode autofluorescence and its use as an indicator of viability. Journal of Nematology 21:399–403.

11. Hussey, R. S., 1989. Disease-inducing secretions of plant-parasitic nematodes. Annual Review of Phytopathology 27:123–141.

12. Hussey, R. S. 1989. Monoclonal antibodies to secretory granules in esophageal glands of *Meloidogyne species*. Journal of Nematology 21:392–398.

13. Hussey, R. S., and C. W. Mims. 1990. Ultrastructure of esophageal glands and their secretory granules in the root-knot nematode *Meloidogyne incognita*. Protoplasma 156:9–18.

14. Hussey, R. S., O. R. Paguio, and F. Seabury. 1990. Localization and purification of a secretory protein from the esophageal glands of *Meloidogyne incognita* with a monoclonal antibody. Phytopathology 80:709–714.

15. Kelly, R. B. 1985. Pathways of protein secretion in eukaryotes. Science 230:25–31.

16. Monck, J. K., and J. M. Fernandez. 1992. The exocyotic fusion pore. Journal of Cell Biology 119: 1395–1404.

17. Nanavati, C., and J. M. Fernandez. 1993. The secretory granule matrix: A fast-acting smart polymer. Science 259:963–965.

18. Perry, R. N., U. Zunke, and U. Wyss. 1989. Observations on the response of the dorsal and subventral oesophageal glands of *Globodera rostochiensis* to hatching stimulation. Revue de Nématologie 12:91–96.

19. Pratzak, A., and H. Winkler. 1986. Exocytotic exposure and recycling of membrane antigens of chromaffin granules: Ultrastructural evaluation after immunolabelling. Journal of Cell Biology 102:510–515.

20. Sheetz, M. P., and J. A. Spudich. 1983. Movement of myosin-coated fluorescent beads on actin cables in vitro. Nature 303:31–35.

21. Shotton, D. M. 1989. Confocal scanning optical microscopy and its applications for biological specimens. Journal of Cell Science 94:175–206.

22. Sundermann, C. A., and R. S. Hussey. 1988. Ultrastructural cytochemistry of secretory granules of esophageal glands of *Meloidogyne incognita*. Journal of Nematology 20:141–149.

23. Takamatsu, T., and S. Fujita. 1988. Microscopic tomography by laser scanning microscopy and its three-dimensional reconstruction. Journal of Microscopy 149:167–174.

24. White, J. G., and W. B. Amos, 1987. Confocal microscopy comes of age. Nature 328:183–184.

25. White, J. G., W. B. Amos, and M. Fordham. 1987. An evaluation of confocal versus conventional imaging of biological structures by fluorescence light microscopy. Journal of Cell Biology 105:41–48.

26. Wyss, U., F. M. W. Grundler, and A. Münch. 1992. The parasitic behaviour of second-stage juveniles of *Meloidogyne incognita* in roots of *Arabidopsis thaliana*. Nematologica 38:98–111.